Chapter 27
Hydraulic Characteristics of the Francis Turbine with Various Groove Shapes of Draft Tube

Hyeon-Seok Seo, Jae-Won Kim and Youn-Jea Kim

Abstract The small hydropower is a renewable energy technology, because the energy resource 'falling water' is replenishable as the fuel (falling water) is part of the hydrological cycle. This technology is being a form of renewable energy with no gaseous emissions, the small hydropower systems are among the options for climate change mitigation and therefore, they are candidates for international carbon trading opportunities such as the Clean Development Mechanism. The draft tube is an important component of a Francis turbine which is one of the small hydropower systems, influences the hydraulic performance. Moreover, as the swirl flow in the draft tube of the Francis turbine decreases pressure at the inlet region, the suppression of swirl flow can be a useful method of minimizing the occurrence of cavitation. In this study, the flow characteristics in a Francis turbine on the 15 MW hydropower generations have been investigated numerically with various shapes of draft tube. Numerical analysis was conducted by using the commercial code, ANSYS CFX. Results showed that the grooved model has relatively uniform distribution of pressure field compared with basic model. Hence, the stability of flow is enhanced, which may attribute to the suppression of draft surge and cavitation.

Keywords Renewable energy · Francis turbine · Groove shapes · Draft tube

Nomenclature

L_d	Length of the cone respectively (mm)
D_{outlet}	Diameter of cone vase of the draft tube (mm)
D_e	Diameter of inlet of draft tube (mm)
U	Velocity (m/s)
P	Pressure (kPa)

H.-S. Seo · Y.-J. Kim (✉)
School of Mechanical Engineering, Sungkyunkwan University,
Suwon 440-746, Korea
e-mail: yjkim@skku.edu

J.-W. Kim
Graduate School of Mechanical Engineering, Sungkyunkwan University,
Suwon 440-746, Korea

X.-R. Zhang and I. Dincer (eds.), *Energy Solutions to Combat Global Warming*,
Lecture Notes in Energy 33, DOI 10.1007/978-3-319-26950-4_27

t Time (s)
k Kinetic energy

Greek Letters
ρ Density (kg/m^3)
μ Viscosity (Pa · s)
ε Dissipation rate

Acronyms
CFD Computer fluid dynamics
RANS Reynolds averaged Navies-stokes
FFT Fast-Fourier transform
FVM Finite volume method
MRF Multiple frame model
SST Shear stress transport

1 Introduction

Hydropower has been a proven, extremely flexible, and well-advanced technology for more than one century. At present, its technology is very mature. Still, there is some room for further improvements. Turbine efficiency is likely the most important factor in a unit. As the heart of the system, design of a turbine is focused on this is to obtain the maximum efficiency. The maximum efficiency can be reached when all losses are kept to a minimum. Hydropower turbines are categorized into two types, which are impulse and reaction turbines, each suitable for different types of water flows and heads. Impulse turbines have simple design and are inexpensive [1]. There are various types of impulse turbines, namely Turgo, Pelton, and cross flow turbines. These types are commonly used as high and medium heads [2]. Recently, they have been applied for lower head microsites, and their proven effectiveness has made them becoming an accepted alternative practice in many countries [3]. Compared to impulse turbines, reaction turbines have a better performance in low head and high flow sites [1, 4]. At slow operating speed, the efficiency of reaction turbines is usually higher than that of impulse turbines [5]. There are also various types of reaction turbines such as propeller or Kaplan, Francis, Pump as, Archimedes screw, and Barker's mill, etc., turbines [6–9].

A Francis turbine is the most commonly used type at hydropower systems [10]. This turbine can be used for micro-, small, medium, or large hydro-systems, as the operating range of Francis turbines is between 1 and 900 m. It has a radial or mixed radial/axial flow runner, which is most commonly mounted in a spiral casing with internal adjustable guide vanes [11]. Flow in the different components of turbine is interrelated and reacts mutually; especially the components like guide vanes, runner, and draft tube have strong influence on one another due to the dynamic forces and resulting vibration. The prediction and understanding of the flow behavior in

casing, runner, and draft tube region hold key importance in redefining the flow and developing better flow techniques to overcome the flow instabilities and the detrimental interaction between the components [12]. While a steady-state analysis using Computational fluid dynamics (CFD) can predict turbine performance parameters like efficiency, cavitation, and hydraulic losses, the analysis of dynamic forces demands calculation of unsteady flow with advanced turbulence model to achieve accurate results. Shear stress model (SST) [13], realizable k-ε [14], standard k-ε including hybrid Kato-Launder correction [15] are of good choices for turbulence model to analyze rotor-stator interaction and pressure pulsation, but more sophisticated turbulence models like Renormalization Group (RNG k-ε) [16, 17], extended k-ε [18], large eddy simulation (LES), scale-adaptive simulation (SAS-SST), Reynolds stress models (RSM) [19] are opted for capturing draft tube vortex rope more accurately. These turbulence models and the numerical simulation as a whole require finer grid, extended computational effort, and CPU time.

The suitable draft tube of a Francis turbine is not determined in the hydropower efficiency and it is necessary to study the effective turbine. Among all hydraulic turbine machines used for energy conversion, extensive operating system of Francis turbine enables it to be used for various ranges of small to large hydropower plant. A draft tube is one of the important parts of a hydro turbine, which is used to transform water into energy. Without a draft tube, the pressure could drop because of lack of water, and in turn, the entire turbine could fail to work and power could be lost. A draft tube can also be either straight or curved, depending on the general construction of the turbine. This makes Francis turbine most popular and hence it is used in large number of hydropower plants. In order to develop a reliable machine for this highly demanding operation, the behavior of the flow in the entire turbine system has predicted a reliable computational method like CFD which is very economical method. Many researchers numerically studied the geometrical effects of blade shapes of the Francis turbine [20, 21]. The result also showed that the change of discharge angle significantly influenced on the performance of the turbine hydraulic efficiency. Wei et al. [22] presented a CFD methodology to study the unsteady rotating vortex in the draft tube of a Francis turbine at part load conditions and associated experimental study of the flow phenomena. They performed unsteady Reynolds averaged Navier-stokes (RANS) simulation for the flow and validated the same with the experimental result. Kurokawa et al. and Qian et al. [23, 24] investigated the possibility of suppressing the draft tube surge in the draft tube of a Francis turbine by using J-groove without decrease of the turbine efficiency. They showed that the change of draft tube significantly influenced on the performance of the hydraulic efficiency. Nishi et al. [25] investigated the three-dimensional (3D) multiphase flow in the Francis turbine. The pressure pulsation in the draft tube, in front runner, guide vanes, and in the spiral case was predicted and analyzed via FFT (Fast Fourier Transform). They showed that the pressure pulsation effected on the performance of the turbine hydraulic efficiency.

Kirschner et al. [26] investigated the water swirling flow in a 9.5° conical diffuser. They showed that the dimensionless peak-to-peak pressure fluctuation and the corresponding dimensionless fundamental frequency were constant with high

cavitation parameter value, but decreased monotonically as the vortex cavitation was developed. Susan-Resiga et al. [27] tried to control vortex with an axial jet in the draft tube. Francis turbine's effectiveness depends on the development of the helical vortex, or the so-called as vortex rope downstream the runner, in the draft tube cone. Resiga et al. [28] proposed a new simple method to reduce the vortex rope by using a water jet supplied with high pressure from the spiral inlet. This had been shown to be able to eliminate the pressure fluctuations at partial load and increase the draft tube efficiency. In the following study, ANSYS CFX software [29] computed the circumferentially averaged flow field, induced the processing vortex rope encountered in the draft tube cone of Francis turbines, worked at partial discharge by using an axisymmetric turbulent swirling flow model.

In this study, the hydraulic performance of a Francis turbine was investigated with two different groove shapes (rectangular and circular) using the commercial code, ANSYS CFX ver. 14.5. In particular, the swirl region and the flow characteristics in the draft tube were studied.

2 Numerical Model

The schematic diagram of a Francis turbine for this simulation is shown in Fig. 1. The modeled Francis turbine was generated through the 2D plan of the Sumjin hydroelectric power plant in Korea. Figure 2 shows the detail view of the draft tube model. The modeled Francis turbine is described as follows: diameter of runner D = 1.4 m, head of Francis turbine H = 151 m, and the rotation speed n = 514 rpm. In addition, it has a runner with 14 blades, a stay vane with 9 blades, a guide vane with 21 blades and 2 gorge shapes of draft tube. The spiral casing of the modeled Francis turbine was fixed for numerical analysis.

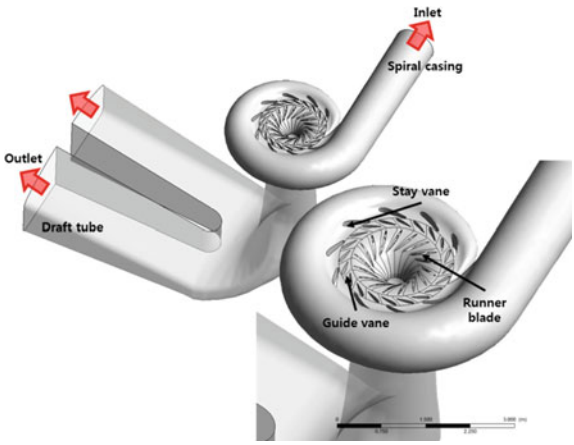

Fig. 1 Schematic diagram of Francis hydraulic turbine

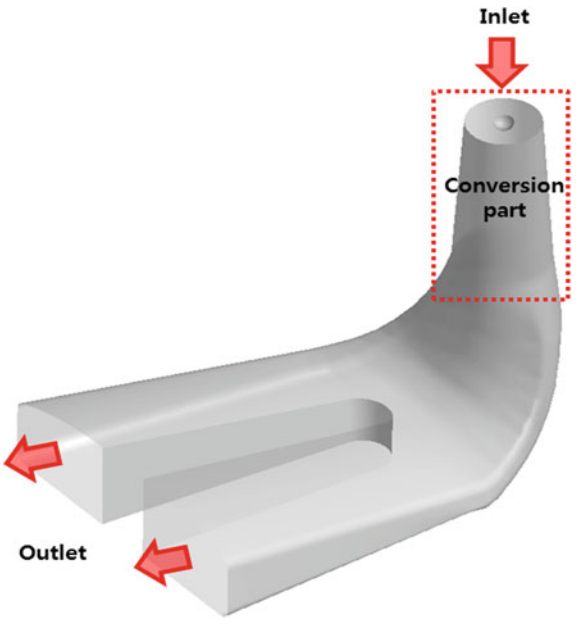

Fig. 2 Detail view of draft tube in Francis turbine

The shape of draft tube is very important part of keeping the stable flow condition as well as to suppress the occurrence of draft surge. Aforementioned, many researchers tried to get the optimum shape of draft tube. In this study, the shapes of draft tube were generated by taking into account of combination with J-groove and O-groove, using the following design criteria [30]:

$$L_d \geq 6(D_{\text{outlet}} - D_e) \tag{1}$$

where D_{outlet} is the diameter of cone base of the draft tube, D_e is the diameter of the inlet of draft tube, and the L_d refers to the length of the cone, respectively. As shown in Fig. 3, the angle of draft tube θ should be less than 5° to satisfy the Eq. (1).

Figure 4 shows the dimensions of the various groove shapes installed in a draft tube of a Francis turbine. In order to control the surge caused by the swirl region in the draft tube, a series of groove (rectangle and circular shapes) were designed on the wall of the inlet of draft tube with the size 1400 mm × 150 mm × 60 mm (Length (L) × width (W) × depth (D)).

We performed a numerical analysis by changing a number of groove from 8–12 which is based on a model acquired by optimum procedure according to the aspect ratio (refer to Table 1).

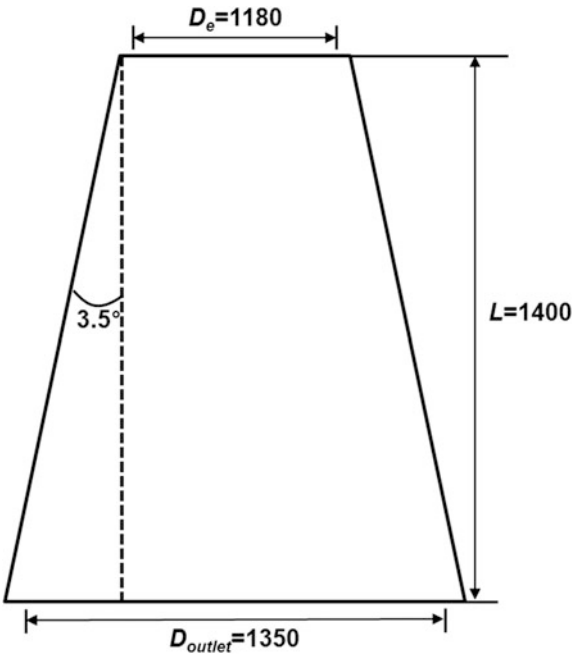

Fig. 3 Dimensions of the draft tube inlet region

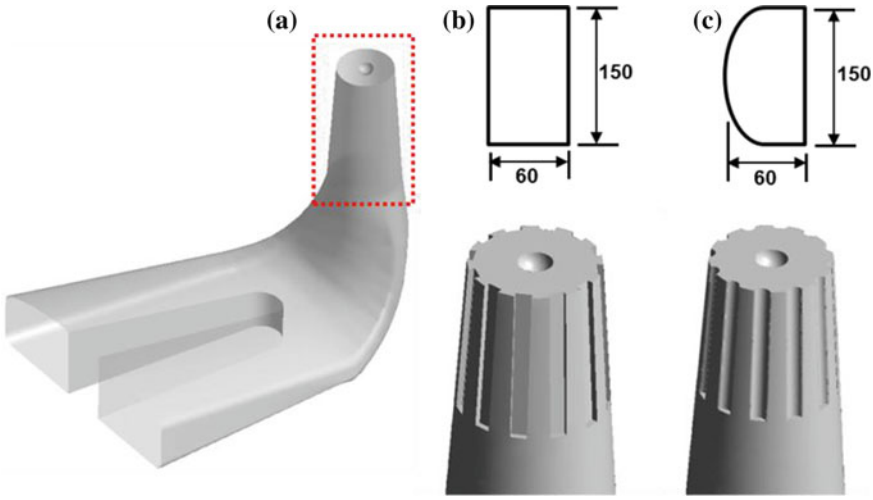

Fig. 4 Groove models applied to draft tube [unit: mm]. **a** Basic model. **b** J-groove. **c** O-groove

Table 1 Draft tube profiles

Types	Groove type	No. of groove
A	Basic model	None
B	J-Groove	8
C		10
D		12
E	O-Groove	8
F		10
G		12

3 Grid Systems and Boundary Conditions

As shown in Fig. 5, 3D discretization has been used with the finite volume method (FVM) provided by the Orieux et al. [31]. In particular, unstructured 3D tetrahedral and hexahedral meshing was employed, due to its flexibility for solving complex geometries.

Table 2 showed the whole number of computational mesh nodes. The irregularity of grids near wall boundary should be thoroughly considered and required the appropriate grid generations for improving the accuracy of the calculated results. In order to investigate the rotating effect of runner blades, the MRF (Multiple Frame Model) method was applied. It is a steady-state approximation where the fluid zone is modeled in a rotating frame of reference and the surrounding zones are modeled

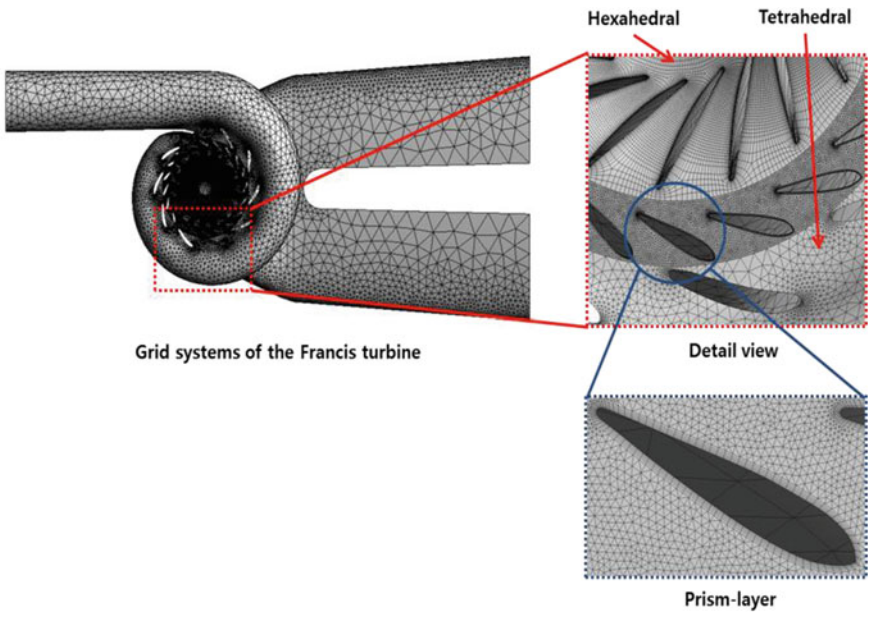

Fig. 5 Grid systems

Table 2 Grid systems of the modeled Francis turbine

Stage	Program	Method	No. of mesh
Spiral casing	CFX	Tetrahedron	1,100,000
Guide vane			110,000
Draft tube			200,000
Runner blade	Turbo grid	Hexahedron	300,000

Table 3 Boundary conditions

Boundary conditions	Value
Inlet of turbine	10.97 (m^3/s)
Outlet of turbine	1 atm
Wall	No-slip wall
Rotor stator interface	Frozen rotor
Calculation type	Steady state
Turbulence model	SST

in a stationary frame. The prism-layer method was applied to individual runner blade, draft tube, and guide vane in order to improve the convergence of numerical calculation. The SST (Shear-Stress-Transport) model was adopted as turbulence model because of its relatively good convergence in the complicated flow field of turbo machinery in comparison with the other models [31]. Table 3 showed the numerical methods and boundary conditions applied in this study.

In general, the numerical results depend upon the solver grid. If the computational resources allow it, it is always recommended to adapt the grid until the solution is independent of the mesh. For CFD analysis, a fine grid resolution in the vicinity of wall is required to obtain a good solution for the boundary layer. Different turbulence models have different dimensionless wall distance (y^+) requirements. It is simply the wall distance times the shear velocity divided by the kinematic viscosity. Also, the y^+ value has a decisive effect on the numerical analysis. For the SST model the requirement is $y^+ < 2$, while for the k-ε model $30 < y^+ < 300$ [31]. We confirmed $y^+ = 1.5$ at the draft tube wall region.

4 Governing Equations

The governing equations for conservation of mass and momentum can be written as follows:

(i) Continuity:

$$\frac{\partial \rho}{\partial t} + \nabla \cdot (\rho U) = 0 \tag{2}$$

(ii) Momentum:

$$\frac{\partial(\rho U)}{\partial t} + \nabla \cdot (\rho U \cdot U) = -\nabla p + \nabla \cdot \tau \tag{3}$$

$$\tau = \mu\left(\nabla U + (\nabla U)^t - \frac{2}{3}\delta \nabla \cdot U\right) \tag{4}$$

where U, p, ρ, and $\nabla(U \cdot \tau)$ are denoted as the velocity, pressure, density, and viscous force, respectively. To consider the turbulent flow in the analysis model, a shear stress transport (SST) turbulence model was employed. The turbulent velocity scale is computed from the turbulent kinetic energy (k). The turbulent length scale is estimated from the two properties of the turbulence field, usually the turbulence kinetic energy and dissipation rate (ε). The turbulence transport term, $\overline{\rho u_i' u_j'}$, can be written as [29]:

$$\overline{\rho u_i' u_j'} = -\mu_t\left\{\frac{2}{3}\delta_{ij}\frac{\partial U_l}{\partial x_l} + \left(\frac{\partial U_i}{\partial U_j} + \frac{\partial U_j}{\partial U_i}\right)\right\} \tag{5}$$

where δ_{ij} is the Konekes delta function, and μ_t is the turbulent viscosity, which is denoted as:

$$\mu_t = \rho C_\mu l_t V_t \tag{6}$$

The velocity and length scales are written as:

$$V_t = \sqrt{k},\ l_t = \frac{k^{2/3}}{\varepsilon} C_\mu \tag{7}$$

The turbulence kinetic energy (k) and the dissipation rate (ε) are written from the transport equations:

$$\frac{\partial(\rho k)}{\partial t} + \frac{\partial\left(\rho \overline{U_j} k\right)}{\partial x_j} = \frac{\partial}{\partial x_j}\left(\Gamma_k \frac{\partial k}{\partial x_j}\right) + P_k - \rho\varepsilon \tag{8}$$

$$\frac{\partial(\rho k)}{\partial t} + \frac{\partial\left(\rho \overline{U_j} \varepsilon\right)}{\partial x_j} = \frac{\partial}{\partial x_j}\left(\Gamma_\varepsilon \frac{\partial \varepsilon}{\partial x_j}\right) + \frac{\varepsilon}{k}(C_{\varepsilon 1} P_k - \rho C_{\varepsilon 2}\varepsilon) \tag{9}$$

where the diffusion coefficients are given by

$$\Gamma_k = \mu + \frac{\mu_t}{\sigma_k},\ \Gamma_\varepsilon = \mu + \frac{\mu_t}{\sigma_\varepsilon} \tag{10}$$

The diffusion rate of the turbulence kinetic energy P_k is given by

$$P_k = -\overline{\rho u_i' u_j'} \frac{\partial \overline{U_i}}{\partial x_j} \tag{11}$$

where the k-ε turbulence model constant C_μ, $C_{\varepsilon 1}$, $C_{\varepsilon 2}$, and ε are 0.09, 1.44, 1.92, and 1.3, respectively. The turbulence model constant for the k equation σ_k is 1. These equations were solved simultaneously by using a commercial CFD code, ANSYS CFX.

5 Results and Discussion

In order to confirm the vortex rope characteristics and hydraulic performance of the Francis turbine, the effects of groove shape (J-groove and O-groove) were investigated. Figure 6 shows the static pressure distributions at the cross section of the modeled draft tube. Results of Type A (basic model) showed that the pressure was increased when the region is away from the inlet of draft tube. Type B–D showed the results of the same region by generating a group of J-groove, and Type E–F for a group of O-groove. Results showed that the J-groove model has relatively uniform distribution of pressure field compared with other types. Consequently, the stability of flow could be enhanced, which may attribute to the suppression of draft surge.

Figure 7 showed the velocity vector distributions at the cross section of draft tube (Type B–D for J-groove, Type E–G for O-groove). Results showed that for a O-groove shape the strength of swirl flow increased to a high level, especially in the region near the wall. Figure 8 showed the detail view of velocity vectors in the

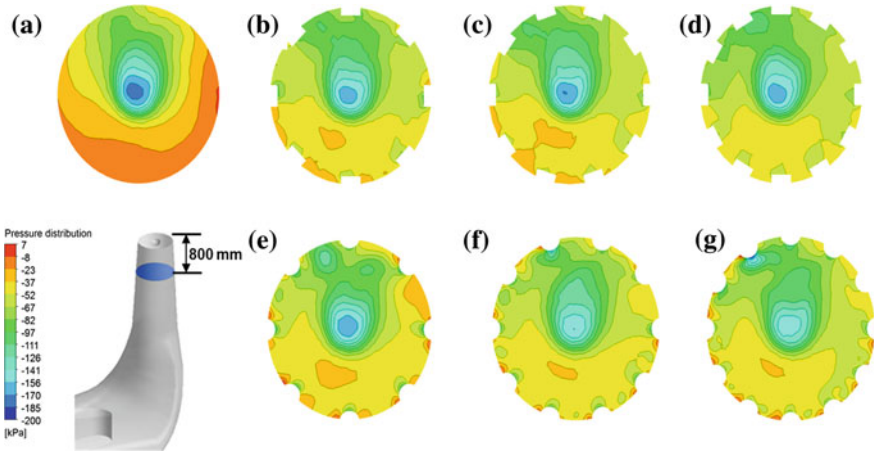

Fig. 6 Pressure distributions at the cross section of the draft tube. **a** Type A. **b** Type B. **c** Type C. **d** Type D. **e** Type E. **f** Type F. **g** Type G

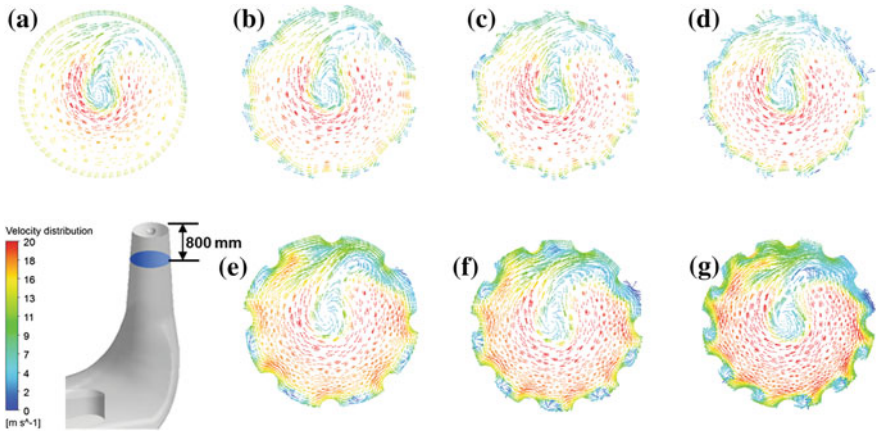

Fig. 7 Velocity vector at the cross section of the draft tube. **a** Type A. **b** Type B. **c** Type C. **d** Type D. **e** Type E. **f** Type F. **g** Type G

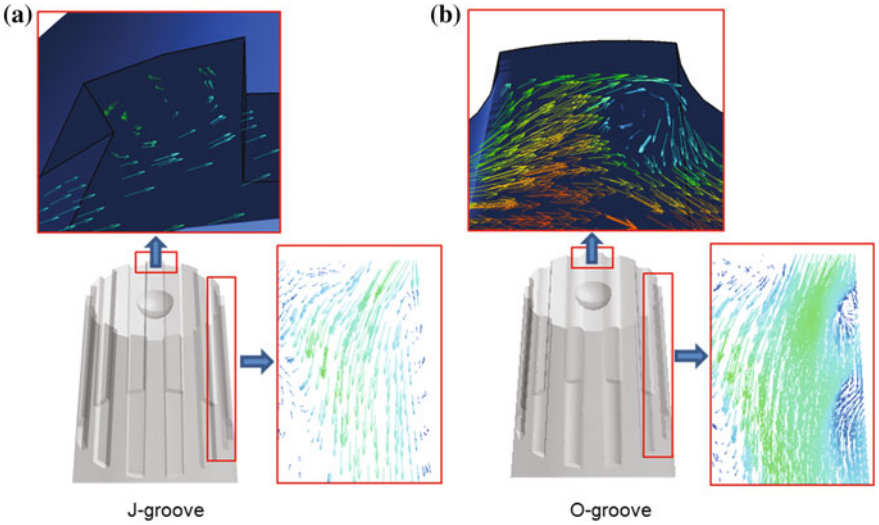

Fig. 8 Detail view of velocity vectors in the passage of J-groove and O-groove

passage of J-groove and O-groove. It is seen that for a J-groove the flow direction shows upward, which is reverse direction to that of main flow in the draft tube. The reverse flow in the passage of J-groove goes out to the center region of draft tube. Therefore, it is conjectured that the strong jet flow from the J-groove to the center region of draft tube performs a role of decreasing circumferential velocity component.

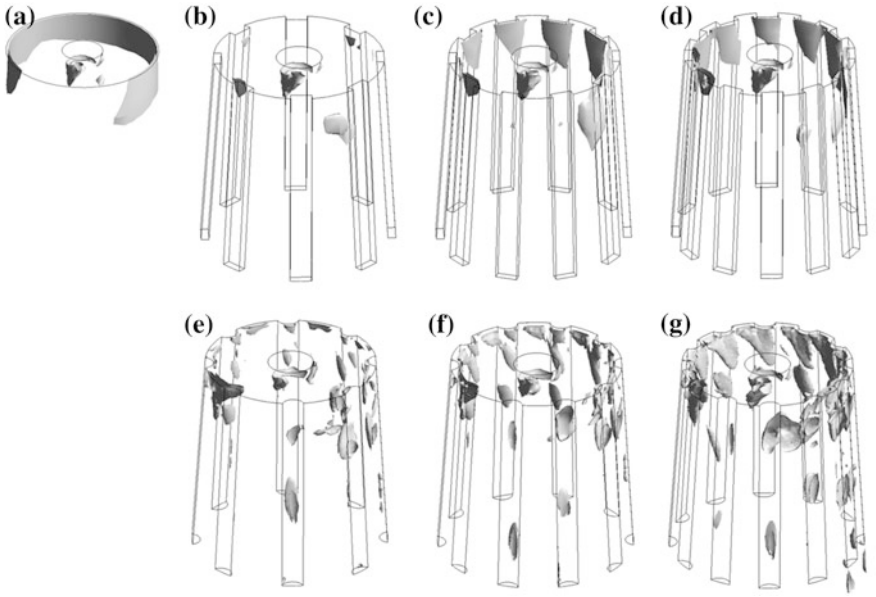

Fig. 9 Vortex core region in the various draft tubes. **a** Type A. **b** Type B. **c** Type C. **d** Type D. **e** Type E. **f** Type F. **g** Type G

A vortex core region in the draft tube also shows that there is high possibility of suppressing draft surge to some extent. The draft surge phenomenon is a result of unstable fluid flow. Main flow is pushed to the region nearby wall surface on the draft tube passage. Figure 9 showed a level of swirling strength which is applied for the observation of vortex core region. Figure 9a showed that in the draft tube basic model, strong whirl flow exists, which may cause draft tube surge. Results also showed that Type B (having J-groove, 8EA) works in good condition with small rotating flow in the draft tube. A strong flow at the center region of draft tube performs a role of decreasing circumferential vortex core. The swirl flow exists far away from the center of draft tube, and the depth of vortex core region is shallow. In order to investigate the effect of groove-shape quantitatively, a comparison of average velocity in the draft tube was carried out between the basic model and groove installation models. Figure 10 shows the average velocity of the axial direction in the draft tube. It is seen that Type B has the lower velocity value than the others. It decreased about 20 % when compared with basic model (Type A). Results also showed that Type G has the high velocity value than the others. It is resulted from the non-uniform internal flow pattern in the draft tube. So these flow patterns when applied J-groove configurations to draft tube provoke the effective pressure recovery performance and these affect to improve the efficiency of turbine system for hydropower production.

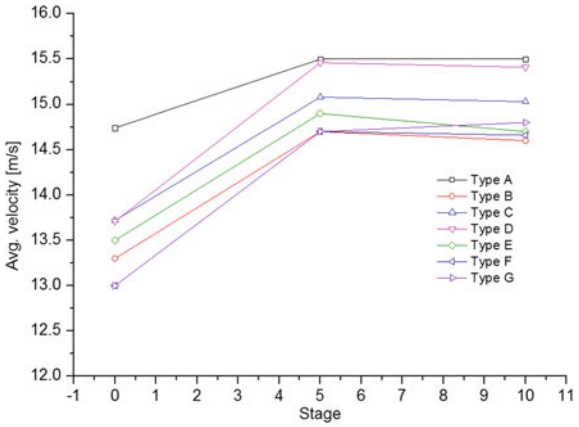

Fig. 10 Average velocity near the wall of draft tube

6 Conclusion

In the present study, the flow characteristic of the Francis turbine has been simulated with various models of draft tube. In order to validate numerical methods, we have compared hydraulic performance values with real operation data obtained from one of the operating hydropower plants in Korea. In particular, the vortex core and pressure distributions in the considered hydraulic turbine were investigated.

Swirl flow from the groove passage to the center region in the draft tube performs a decisive role of increasing circumferential pressure component. Therefore, vortex core region diminished considerably with the groove shapes on the wall of the draft tube. The Francis turbine with Type B (J-groove, 8EA) represents the best result among the various model cases that showed a small swirl flow in the draft tube.

From the continued following study for the shape optimization of J-groove, further improvement of suppression performance for the swirl flow in draft tube will be expected. For better understanding of this fascinating flow problem, however, it may be necessary to perform the experimental works. In the near future, we would be glad to compare these numerical results with those obtained by anyone in the same field.

Optimization of the small hydropower systems considering various design factors such as guide vane, impeller, casing, and draft tube configurations, etc., and topographic characteristics will make more promising than purely optimization of structures. From now on, optimization of operating conditions, mitigating or reducing environmental impacts, adapting to new social and environmental requirements and more cost-effective technological solutions are more and more important. Such as hydrokinetic turbines, or hybrid windhydropower turbine systems, etc., with the application of new technologies, the new styles of turbines are more efficient and environmentally friendly, and can compete with traditional designs.

References

1. Edy EJ (2009) Final study report, achievable renewable energy targets for Puerto Rico's renewable energy portfolio standard. Puerto Rico's Energy Affairs Administration, Puerto Rico. (Chapter 8)
2. Paish O (2002) Small hydro power: technology and current status. Renew Sustain Energy Rev 6:537–556
3. Wallace AR, Whittington HW (2008) Performance prediction of standardized impulse turbines for micro-hydro. Elsevier B.V., UK (Sutton, Int Water Power Dam Constr)
4. Ghosh TK, Prelas MA (2011) Energy resources and systems. In: Renewable resources, vol 2. Springer, Dordrecht
5. Miller G, Corren D, Armstrong P, Franceschi J (1987) A study of an axial-flow turbine for kinetic hydro power generation. Energy 12(2):155–162. Great Britain Pergamon Journals Ltd
6. Agarwal T (2012) Review of pump as turbine (PAT) for micro-hydropower. Int J Emerg Technol Adv Eng 2(11):163
7. Ramos H, Borga A (1999) Pumps as turbines: an unconventional solution to energy production. Urban Water 1:261–263
8. Date A, Date A, Akbarzadeh A (2013) Investigating the potential for using a simple water reaction turbine for power production from low head hydro resources. Energy Conv Manag 66:257–270
9. Okot DK (2013) Review of small hydropower technology. Renew Sustain Energy Rev 26:515–520
10. Voith-Siemens (2013) Francis turbines, hydropower generation, Voith. http://voith.com/en/Voith_Francis_turbines.pdf. Accessed 15 Aug 13
11. Kc A, Thapa B, Lee Y (2014) Transient numerical analysis of rotor-stator interaction in a Francis turbine. Renew Energy 65:227–235
12. Benigni H, Jaberg H (2007) Stationary and transient numerical simulation of a bulb turbine. In: 5th IASME/WSEAS international conference on fluid machineries and aerodynamics, pp 135–140
13. Qian ZD, Zheng B, Huai WX, Lee YH (2009) Analysis of pressure oscillations in a Francis hydraulic turbine with misaligned guide vanes. Proc Inst Mech Eng Part A J Power Energy 224:139–152
14. Ruprecht A, Heitele M, Helmrich T (2000) Numerical simulation of a complete francis turbine including unsteady rotor/stator interactions. Inst Fluid Mech Hydraul Mach
15. Ying H, Heming C, Ji H, Xirong L (2011) Numerical simulation of unsteady turbulent flow through a Francis turbine. J Nat Sci 16(2):179–184
16. Li J, Yu J, Wu Y (2010) 3D unsteady turbulent simulations for transients of the Francis turbine. In: 25th IAHR symposium of hydraulic machinery and systems. IOP conference series: earth and environmental science, p 12
17. Ruprecht A, Helmrich T, Aschenbrenner T, Scherer T (2002) Simulation of vortex rope in a turbine draft tube. In: Proceedings of the hydraulic machinery and systems 21st IAHR symposium
18. Jost D, Lipej A (2011) Numerical prediction of non-cavitating and cavitating vortex rope in Francis turbine draft tube. J Mech Eng 57(6):445–456
19. United States Department of the Interior, Bureau of Reclamation (1976) Selecting hydraulic reaction turbines. Engineering monograph, No 20
20. Sayers AT (1990) Hydraulic and compressible flow turbo machine. McGraw-Hill, New York
21. Cioacan GD, Iliescu MS, Vu TC, Nennemann B, Avellan F (2007) Experimental study and numerical simulation of the FLINDT draft tube rotating vortex. ASME J Fluids Eng 129:146–158
22. Wei Q, Zhu B, Choi YD (2012) Internal flow characteristics in the draft tube of a Francis turbine. J KSME 36:618–626

23. Kurokawa J, Imamura H, Choi YD (2010) Effect of groove on the suppression of swirl flow in a conical diffuser. ASME J Fluids Eng 132:071101-1–071101-8
24. Qian ZD, Yang JD, Huai WX (2007) Numerical simulation and analysis of pressure pulsation in Francis hydraulic turbine with air admission. J Hydrodyn 19:467–472
25. Nishi M, Wang XM, Yoshida K, Takahashi T, Tsukamoto T (1996) An experimental study on fins, their role in control of the draft tube surging. In: Proceedings of the 17th IAHR symposium, pp 905–914
26. Kirschner O, Schmidt H, Ruprecht A, Mader R, Meuburger P (2010) IOP conference on earth and environmental science, p 012092
27. Susan-Resiga R, Thi CV, Sebastian M, Ciocan GD, Nennemann B (2006) Jet control of the draft tube vortex rope in Francis turbines at partial discharge. In: Proceedings of the 23rd IAHR symposium, vol 1, p 14
28. Susan-Resiga R, Sebastian MPS, Francois A (2008) Axisymmetric Swirling flow simulation of the draft tube vortex in Francis turbines at partial discharge. In: Proceedings of the 24th symposium on hydraulic machinery and systems, IAHR, pp 27–31
29. ANSYS Corporation CFX ver. 14.5 Manual (2014)
30. Menter FR (2012) Two-equation eddy-viscosity turbulence models for engineering applications. J AIAA 32:1598–1605
31. Orieux S, Rossi C, Esteve D (2002) Thrust stand for ground tests of solid propellant microthrusters. Rev Sci Instrum 73:2694–2699